Rodríguez-Millán, M.,Díaz-Álvarez, A., Aranda-Ruiz, J., Díaz-Álvarez, J. y Loya, J.A. (2019). Experimental analysis for stabbing resistance of different aramid composite architectures, *Composite Structures*, 208, pp. 525-534.

DOI: https://doi.org/10.1016/j.compstruct.2018.10.042

Funding: Ministry of Economy and Competitiveness of Spain and FEDER program under the Project RTC-2015-3887-8 and the Project DPI2017-88166-R

Experimental analysis for stabbing resistance of different aramid composite architectures

M. Rodríguez-Millán[a,*], A. Díaz-Álvarez[a], J. Aranda-Ruiz[b], J. Díaz-Álvarez[a], J.A. Loya[b]

[a] Department of Mechanical Engineering, University Carlos III of Madrid, Avda. de la Universidad 30, 28911Leganés, Madrid, Spain
[b] Department of Continuum Mechanics and Structural Analysis, University Carlos III of Madrid, Avda. de la Universidad 30, 28911Leganés, Madrid, Spain

A B S T R A C T

Stab resistance is a crucial material property in the case of fabrics used in personal protection equipment due to the extensive occurrence of this threat. Personal Protection Equipments (PPE) are commonly based on woven aramids, where the stacking sequence is critical to improve the ratio between protection and weight. PPE should combine optimal penetration resistance with ergonomic requirements. This paper focuses on experimental characterisation of the stab protective efficiency of different architectures of aramid laminates. The influence of different stacking sequences, based on the combination of not treated (N) and thermoplastic aramids (TP), is analysed showing a significant influence of this factor. In the range of the impact energies analysed in this work, it can be concluded that the TP-N-TP sequence is the best choice for stabbing protection.

Keywords:
Experimental characterisation
Stabbing
Trauma
Aramid laminate

1. Introduction

Currently, knives and other sharp objects are commonly used in assaults due to the restrictions imposed by gun control legislation, especially in Europe and Asia. The knife wound is an essential societal problem because of the frequent occurrence of this type of lesion for both security members and civilian population, thus leading to an increase in stab protection demand. Therefore, fabrics used in PPE for law enforcement agents should be designed accounting for both possible threats: ballistic impact and slash or knife penetration.

PPE is commonly based on aramid fibres (for instance, commercial material Kevlar® is a para-aramid while Nomex® is a meta-aramid) and ultra-high molecular weight polyethene (UHMWPE) fibres because of their high resistance against high energy projectiles and excellent cut resistance. The layers are stacked to achieve protection requirements, and sometimes they are combined with a polymeric matrix constituting a composite material. The performance of these types of materials has been widely analysed in the literature mainly for ballistic applications [1–6]. However, protections should also provide stab resistance, and in general, the optimised configuration for ballistic resistance is not the better solution for stabbing [7,8]. Different authors have focused explicitly on stabbing resistance analysis based on experimental approaches as well as numerical and analytical modelling [9–16].

Stabbing resistance depends on the yarn count and mechanical properties such as friction, stretching, breakage resistance, the weave architecture and the fabric density. The hazard is related to the size and shape of the knife and the impact energy. The damage caused by knife attack on apparel is strongly related to the perpetrator characteristics (such as gender, corpulence, and previous training) as it was demonstrated in a recent study of Cowper et al. [9].

It is commonly accepted that textile stabbing involves three different steps: the initial penetration step, the second cutting step caused by a knife edge, and the third step leading to the destruction of the assembled fibre bundle, as it is explained in a recent work of Hejazi et al. [10]. These authors proposed a novel woven textile coated with a series of metals for stab-resistant protective clothing (PC) developing a mechanical model to indicate the textile and blade parameters are influencing the resistant of PC under vertical stabbing [10].

Modifications to the basic scheme of composite laminates for protections have been recently achieved to improve stabbing performance and comfort. For instance, Reiners et al. [11] demonstrated that the insertion of a wool layer diminishes the number of layers with acceptable stab depth values. The main advantage is weight reduction and improved wear comfort because of the softer structure. The relationship between the number of layers in a protective package and depth of penetration on the protection was studied by Barnat et al. [12]. As it was expected, the number of layers of the protective package is a crucial element in the study of stab resistance.

The improvement of the stab resistance in high-performance fabrics has also been approached through the incorporation of polymer

Nomenclature

PC	protective clothing
TP	thermoplastic-impregnated aramid
N	not treated aramid
DOP	depth of penetration
RDOP	relative depth of penetration
D_0	length of depth of penetration without protection
D_1	length of depth of penetration with protection consisting of three different layers
ρ_g	density of the gelatine
ρ_p	density of the protection consisting of different layers
t_p	total thickness of the protection consisting of different layers
E_c	impact energy
E_S	specific energy absorption, units: $\left(\frac{J}{g/cm^2}\right)$
SEM	Scanning Electronic Microscope

coatings or laminated films into woven fabrics, such as thermoplastic-impregnated aramid (TP) or shear thickening fluids (STFs). The polymer matrix improves the woven fabrics toughness [14] leading to increased levels of energy required to cut and separate fibres and yarns.

Thermoplastic-impregnated aramid (TP) is an excellent choice for stabbing protections, however, this type of protective material has not been widely analysed in the literature. Studies carried out by Mayo et al. [14], Hosur et al. [15], and Rao et al. [17], among others, revealed that TP-aramid shows good stab resistance proving the possibility to be used in PPE applications. Hosur et al. [15] performed static and dynamic tests to evaluate stab resistance properties of TP-Kevlar composites obtaining good resistance, especially in the case of quasi-static spiking. Mayo et al. [14] characterised thermoplastic-impregnated aramid fabrics under static and dynamic stab and puncture testing. The results demonstrated that the stab resistance of aramid fabrics could be enhanced through the incorporation of thermoplastic films. Stab characterisation of hybrid ballistic fabrics consisting of TP-Kevlar, STF-Kevlar and not treated Kevlar was developed by Rao et al. [17]. They found that not treated Kevlar exhibited the lowest resistance in both dynamic and quasi-static spike testing while the use of TP-Kevlar improved the performance of all the fabrics.

Despite the previous effort of different authors stabbing is still an active field of research. The importance of combining both stabbing and ballistic resistance is mentioned in most papers, but it is challenging to find analysis of different laminate architectures proper for both threats. Ballistic resistance is commonly achieved with dry layers of fibres leading to flexible protections avoiding transfer of energy in a narrow zone. Flexible protections are also related to better ergonomic performance. However, the improved behaviour of TP aramid under stabbing indicates that not treated layers could not be the best anti-stabbing solution.

The mechanical response of vest armor protections, that use to consists of inserts of 20–50 layers of para-aramid textiles [18], depends of the lay-up sequence. For this reason, a small-scale in-depth study of different combinations of two types of aramids commonly used in vests against stabbing is conducted this work. Due to the reduced number of layers in comparison with the current standards recommendation, stabbing test were performed following a specific experimental procedure. For a complete analysis of the vest, a larger scale study would be necessary. The results obtained here can give relevant information to manufacturers on the use of untreated and treated aramid fibres.

The optimisation of the stacking sequence for a threat requires previous analysis of the stabbing resistance contribution of a single layer. For this reason, in this paper, three different stacking sequences (architectures), involving not treated and thermoplastic-impregnated woven aramid layers (N- aramid and TP- aramid, respectively), are analysed under stabbing threat. The investigation reported in the present paper is precise of this nature. Firstly, experimental tests are conducted on laminates and, secondly, the results are shown and analysed. The analysis of performance architecture is carried out regarding the depth of penetration (DOP), absorbed energy, impact force and damaged area. From the analysis emerges a central idea, which is the main innovative feature of this paper: to evaluate personal protection against stabbing regarding a single analysis variable does not guarantee optimal protection. Therefore, significant differences regarding the depth of penetration, energy absorption, medium impact force and damage observations were found between the different architectures analysed.

2. Experimental methodology for stabbing analysis

2.1. Materials

Three stacking sequences involving two different types of fabric layers are studied in this work: thermoplastic-impregnated aramid (TP-aramid) and not treated woven aramid (N- aramid). Regarding yarn count, both aramid types present similar architecture (see Table 1 for details). The main difference relies on the presence of the thermoplastic matrix in TP-aramid, leading to a rigid configuration, higher thickness and areal density 55% greater than in N-aramid, presenting a flexible configuration.

Three different symmetric combinations *3TP, TP-N-TP, N-TP-N* are considered involving a combination of three TP and N aramid layers. Details of each architecture, as the areal density, total thickness and mass of each stacking sequence are included in Table 2. Note that the *3N* configuration has not been analysed, due to the null resistance to stabbing, as it is a flexible fabric configuration.

2.2. Experimental set up

Dynamic stabbing resistance is evaluated using a drop-weight tower (INSTRON CEAST Fractovis 6785, Fig. 1a). The impact test is based on the free-fall of a known mass impactor, detailed in Fig. 1b), which provides the energy required to stab the specimen.

Following the NIJ Standard 0115.00 [19], a particular purpose tool has been designed (see Fig. 2) to grip a given HOSDB/S1/G sharpness blade to the impactor-end. The kinetic energy of the impactor can be adjusted varying the drop-height being the total mass of the system 4.485 kg.

To determine the specimen stabbing resistance, tests were performed in the range 0–140 mm free-falling striker height leading to a range of 0–6.5 J impact energy. Note that this energy is lower than that considered in the standards of personal protection analysis, this is because, in this work, 3 sheets of aramid are analysed and not a real vest.

Stabbing tests were carried out on 160 × 160 mm aramid sheets. The specimen sheets were fixed using a steel-frame clamping 25 mm in the perimeter, resulting in a 110 × 110 mm impact surface (see Fig. 3),

Table 1
Not treated and thermoplastic aramid fabric layers' characteristics.

Material	Weave type	Areal density (g/m^2)	Yarn count Warp/Weft ($Ends/cm$)	Thickness (μm)
Not treated aramid (N-aramid)	Plain	190.4	10.7 × 10.7	310
Thermoplastic aramid (TP-aramid)	Plain	317	10.5 × 10.5	250

Table 2
Architecture of different analysed sequences.

Nomenclature	Layer combination	Areal density (g/m^2)	$t(mm)$	mass (g)
3TP	*3 sheets of TP-aramid*	*952.6*	*0.75*	*21.43*
TP-N-TP	*2 sheets of TP-aramid and 1 sheet of N-aramid*	*698.4*	*0.81*	*18.57*
N-TP-N	*1 sheet of TP-aramid and 2 sheets of N-aramid*	*825.5*	*0.87*	*15.71*

with the gelatine block contacting the backing material. The targets were aligned with the striker to receive the impact in the centre of the sheets. Once the striker was positioned at the corresponding initial height to achieve the desired impact energy, it dropped in a free-falling process.

2.3. Backing material

Gelita gelatine Type Ballistic 3 (10% concentration mass ratio) was used as the backing material because it allows to easily obtain the depth of penetration. Following the manufacturer's instructions, the mix of gelatine powder and cold water was cooked in a double boiler heating arrangement heated to temperatures below 60 °C to avoid gelatine degradation. Slow stirring during the process was necessary to avoid air bubbles, leading to a similar mix time.

Silicon moulds are filled w ith g elatine t o o btain g elatin cubes ($100 \times 100 \times 100\,mm^3$). Once the gelatine blocks solidify, they are unmolded. To preserve the humidity of the blocks, they are protected with transparent film and stored at 4C. in a refrigerator until the test stabbing is carried out (Fig. 4). The whole cooking process per block took 2 h approximately, followed by an additional solidification time into the moulds close to 12 h.

Due to the transparency of the gelatine, the trauma caused by the stab can be directly measured by visual inspection, as can be seen in Fig. 5. To measure the trauma, the contrast is improved injecting blue-ink into the stab (see Fig. 5a). This methodology allows to obtain measurements with errors less than 1 mm.

The interesting parameters are the depth of penetration (DOP), the relative depth of penetration (RDOP), the energy absorbed by the laminate (E_{abs}), the specific energy absorbed by the laminate (E_{spec}), the specific i mpact f orce (F) a nd d amage a rea. E ach o f t he parameters studied are defined below.

The depth of penetration (DOP) to quantify the stabbing trauma and is defined as the distance between the top surface of the gelatine and the front tip of the blade penetrating the gelatine through the aramid laminate (see Fig. 5b).

To take into account the weight (areal density) in the efficiency of the armour, the use of residual depth of penetration (RDOP) is proposed. This parameter, commonly used to evaluate the ballistic efficiency of armour [20], is given in the following the equation:

$$RDOP = \frac{(DOP_0 - DOP_1)\rho_g}{t_p \cdot \rho_p} \tag{1}$$

being DOP_0 the DOP without protection (considering just the gelatine block), $DOP_1$with protection, ρ_g the density of the gelatine, ρ_p the equivalent density of the stack protection, and t_p the total thickness of the combination of the three layers.

The energy absorbed by the laminate is estimated and compared to the energy absorbed by the gelatine block without protection which is assumed to be proportional to the DOP. Thus, the energy absorbed by the laminate, E_{abs}, can be defined in Eq. (2):

$$E_{abs} = E_c\left(\frac{DOP_0 - DOP_1}{DOP_0}\right) \tag{2}$$

where the impact energy is E_c, DOP_1 and DOP_0 corresponds to the case with and without protection respectively. Therefore, the better is the protection efficiency, the higher is the difference ($DOP_0 - DOP_1$) and, ideally, $E_{abs} \rightarrow E_c$. The specific energy absorbed by the laminate is defined as the ratio between the absorbed energy and their areal density.

An equivalent mean impact force can be estimated as the ratio between impact energy, E_c and depth of penetration, DOP , according to [11]. The specific mean impact force, or *Specific force*, is determined by dividing the mean impact force by the corresponding laminate density.

The damaged area measurement is obtained from the images of the OPTICA SZR camera. The damaged area is assumed to be a rectangle formed by the crack in x and y directions.

3. Results and discussion

In this section, material performance is evaluated regarding the depth of penetration, energy absorption, mean impact forces and puncture damage morphology. The different weights of each configuration have also been considered, including this factor in the corresponding normalised variables.

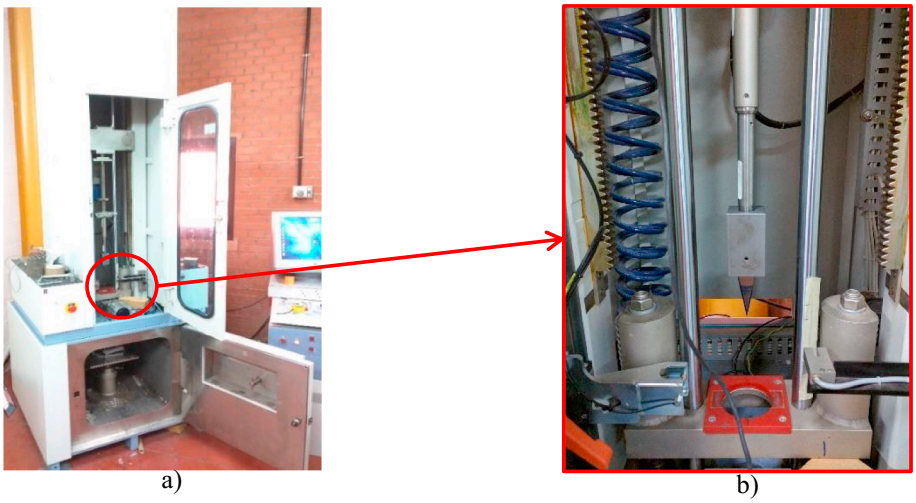

Fig. 1. INSTRON CEAST Fractovis 6785. a) General view and b) detail of the stab impactor.

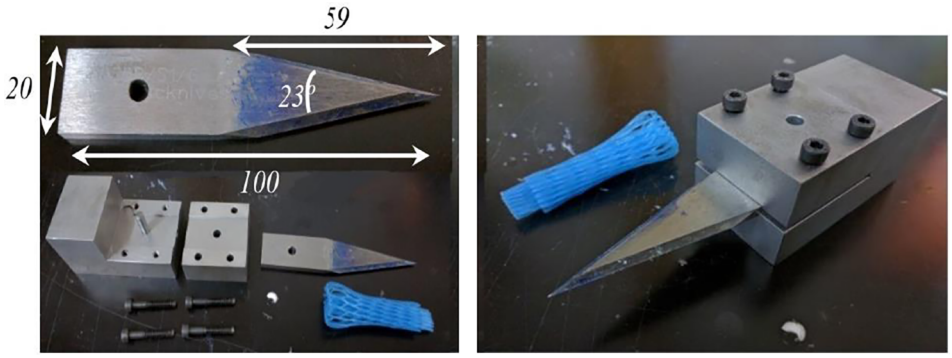

Fig. 2. Adapting striker-to-blade aluminium tool.

3.1. Depth of penetration

DOP obtained for a wide range of 0.2–6.5 J impact energies is presented in Fig. 6. More than 20 tests were performed for each laminate configuration. In the range of energies analysed no penetration was observed below 0.2 J, and penetration was reached above 6.5 J in all cases.

The depth of penetration into the backing material increased with the impact energy as it is expected. In general, the 3TP architecture exhibits higher stab resistance against penetration when compared to the other laminates, especially at low impact energies (below 4.5–5 J, approximately). N-TP-N hybrid composite reaches elevated *DOP* at 3.4 J, while the other configurations present much lower values of DOP up to 5.7 J. The DOP_{max} is close to 39 mm for all configurations; however, the energy level at this value is significantly larger for 3TP composite. The onset of penetration also occurs for higher energy values in the case of 3TP composite (around 1.7 J) showing the best behaviour under stabbing of this architecture.

DOP is strongly dependent on the fabric density. Larger fabric density led to a steep decrease in penetration depth, see [11,14,21]. For low impact energies (below 2 J), 3TP aramid laminate seems to be the best configuration for personal protection equipment (PPE). DOP is significantly lower (around 4 times) than that obtained in other configurations; however, the areal density of 3TP is the highest, (11% and 25% higher than TP-N-TP and N-TP-N cases, respectively). For moderate values of impact energy (between 1.5 and 4 J), the configuration N-TP-N aramid presents the maximum value of DOP.

The variation in RDOP vs impact energy is presented in Fig. 7. Comparing to the previous figure, the differences between different stack configurations decrease when normalised DOP is used. It can be appreciated that the 3TP combination, which energy at the penetration onset is the highest, presents the higher efficiency up to close 5 J (higher RDOP). Moreover, TP-N-TP hybrid composite is found to offer better protection than N-TP-N hybrid composite. The differences

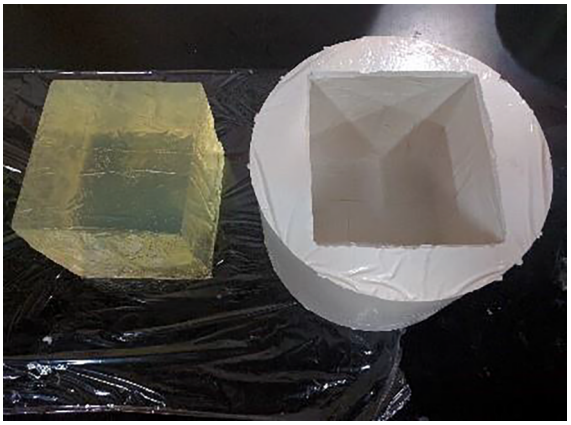

Fig. 4. Manufactured gelatine block (left) and silicon mould (right).

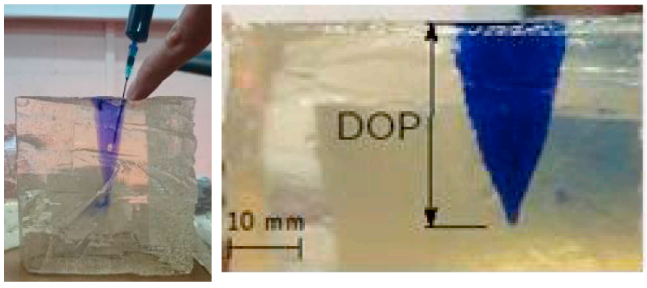

Fig. 5. a) Ink injection to improve contrast; b) Example of an impacted gelatine block. The DOP = depth of penetration.

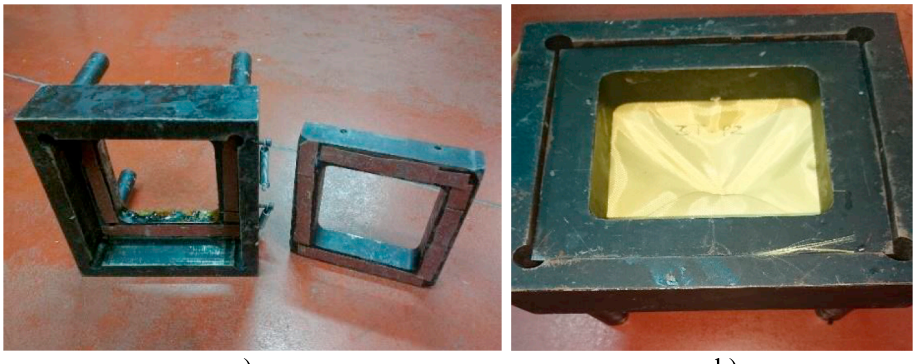

Fig. 3. a) Steel-frame to fix aramid sheets; b) Frame with the tested specimen (right).

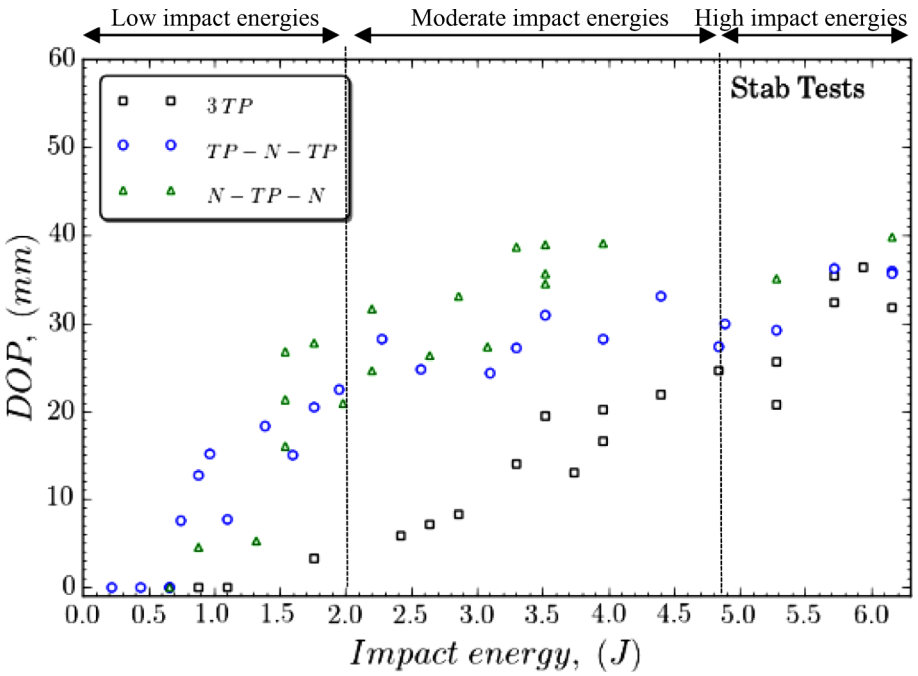

Fig. 6. DOP vs impact energy.

between the three configurations become significantly reduced at high impact energies (around 5 J).

Therefore, for both penetration parameters, DOP and RDOP, the best configuration is 3TP configuration; although for high impact energies, this improvement is negligible concerning the TP-N-TP configuration. A summary of the results in this section is shown in Table 3.

3.2. Energy absorption

The energy absorbed by the laminates vs impact energy is presented in Fig. 8. The N-TP-N hybrid composite is found to offer the worst effective protection within the whole range of impact energies tested whereas the 3TP configuration presents the highest level of energy absorption.

The ratio between the absorbed energy and their areal density are summarized in Table 4 for all cases. The best configuration is TP-N-TP hybrid composite from the point of view of energy absorption in stabbing tests for high impact energy (6.2 J), and it is around 17% higher than that exhibited by the 3TP hybrid composite.

If energy parameters are used as a reference, conclusions are partially similar to those observed in the case of DOP analysis. At low and moderate impact energies, the 3TP configuration presented the best stabbing behaviour, slightly better than the TP-N-TP configuration; however, at high impact energy values and taking into account the weight of the laminate; it is found that the best configuration is formed by TP-N-TP.

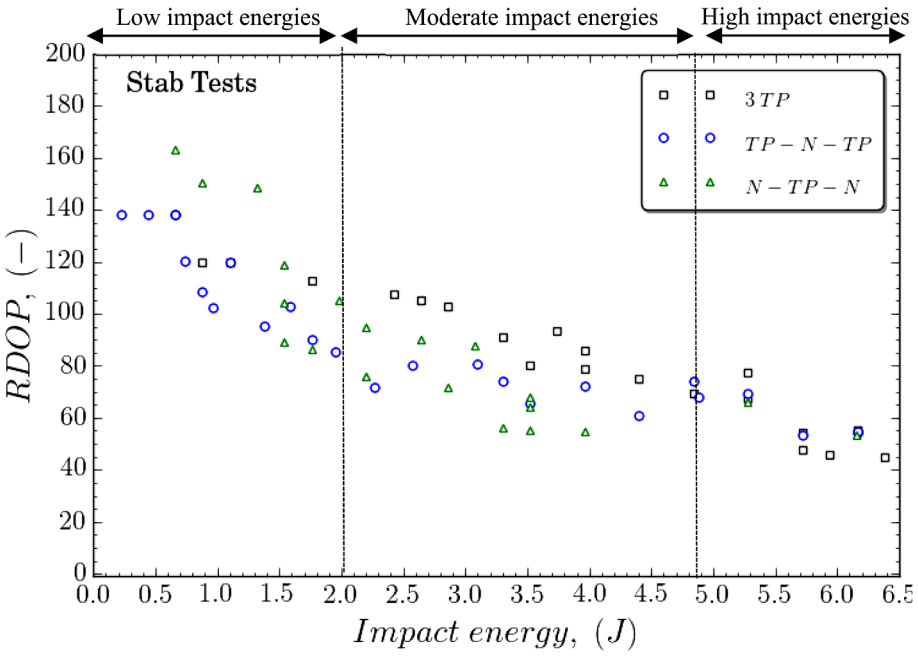

Fig. 7. RDOP vs impact energy.

Table 3
Comparison of DOP and RDOP.

Test	3 TP-aramid ($\rho_{areal} = 0.0952 g/cm^2$)		TP-N-TP aramid ($\rho_{areal} = 0.0698 g/cm^2$)		N-TP-N aramid ($\rho_{areal} = 0.0825 g/cm^2$)	
	DOP (mm)	RDOP (–)	DOP (mm)	RDOP (–)	DOP (mm)	RDOP (–)
Moderate impact energy (2.4 J)	5.96	107.57	28.28	71.89	31.6	75.79
High impact energy (6.2 J)	36.96	55.1	35.89	54.08	39.76	53.22

3.3. Mean impact force to inflict the stab wound

The force level required to inflict the stab wound is a critical parameter in stabbing events. The mean force constitutes a parameter quantifying the efficiency of the protection. Larger values of the mean force indicate the higher ability of the protection to stop more aggressive impact (larger reaction forces) for smaller values of the penetration.

The specific mean impact force, or *Specific force*, is determined by dividing the mean impact force by the corresponding laminate areal density. When it is represented vs the impact energy (Fig. 9), it is observed that the specific force for 3TP remains higher at moderate impact energies and similar to values at high impact energies when compared with the specific force for 3TP and N-TP-N. However, the specific force significantly decreases for 3TP composite with impact energy, while it slightly increases for the other configurations. The decrease in penetration force between low impact energy and high impact energy can be explained by the effect of thermoplastic that impregnates the aramid because the TP-aramid resulting weakened at higher velocities. Due to the TP-aramid weakening at the point of contact with the blade, the energy release rate increases, allowing the crack to propagate through the material more efficiently, resulting in a reduced rupture force. The presence of N aramid counteracts this phenomenon because of the nature of this flexible layer. Thus, forces increase with absorbed energy when N aramid is included in the protection architecture. A summary of the results is shown in Table 5.

In Fig. 10, the specific impact force is represented vs DOP. For low values of penetration, 3TP composite needs more specific impact force than others; however, for high values of penetration all configurations analysed present similar behaviour.

At this point, it is quite clear that the 3 TP configuration has the better stabbing performance for low and medium impact energies. However, at high impact energies, both the 3TP configuration and the TP-N-TP laminate present similar capabilities for the same areal density level. In this case, using the specific force as the design variable, the TP-N-TP laminate can be considered the best design option because it exhibits a higher specific force value and lower DOP value.

3.4. Puncture damage observations

Protection damage was analysed using an OPTICA SZR camera and a Scanning Electronic Microscope (SEM) to observe the fibre damage in detail and improve the understanding of the failure mechanisms during stabbing tests. The damaged area in each layer was analysed for different configurations. Different damage mechanisms can be distinguished depending on the impact energy and the layout observed:

Damage caused in N-aramid is shown in Fig. 11. This figure shows a postmortem picture of specimens obtained using the OPTICA SZR camera and a detail of the cutting area using SEM. Three main failure mechanisms are identified:

- *Cutting yarns:* This is the primary failure mechanism; however, the number of cut yarns depends on impact energy as can be seen in Fig. 11a (left) and Fig. 11c. Fig. 11a (left) is a picture of the damaged area at impact energy = 0.88 J. Local tearing strength of fibres is exceeded by the impact force, and therefore, the fibres are cut. The-

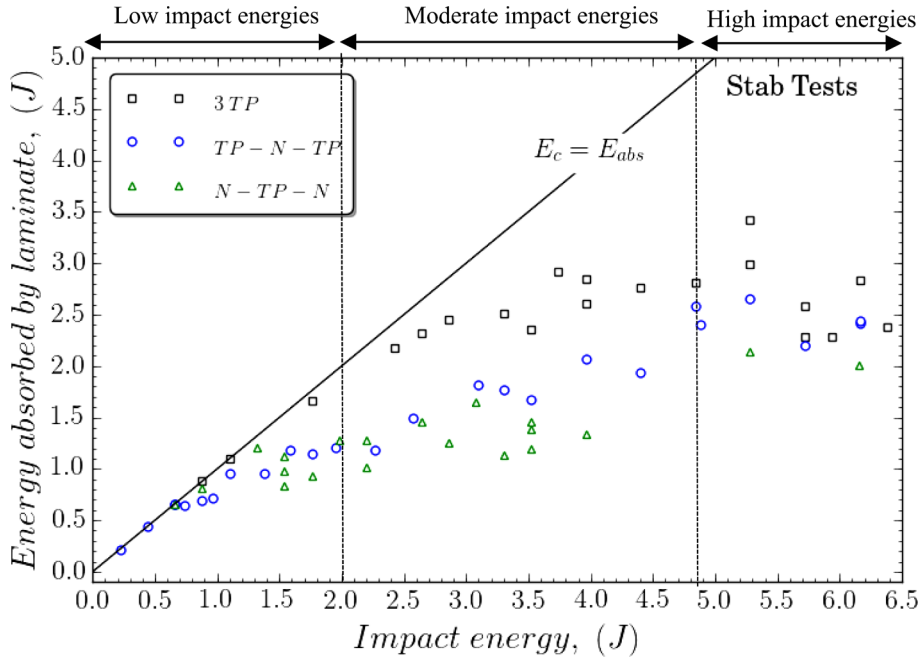

Fig. 8. Energy absorbed by laminate vs impact energy.

Table 4
Comparison of energy absorbed and specific energy.

Test	3 TP-aramid ($\rho_{areal} = 0.0952 g/cm^2$)		TP-N-TP aramid ($\rho_{areal} = 0.0698 g/cm^2$)		N-TP-N aramid ($\rho_{areal} = 0.0825 g/cm^2$)	
	Energy abs. (J)	Specific energy $\left(\frac{J}{g/cm^2}\right)$	Energy abs. (J)	Specific energy $\left(\frac{J}{g/cm^2}\right)$	Energy abs. (J)	Specific energy $\left(\frac{J}{g/cm^2}\right)$
Moderate impact energy (2.4 J)	2.17	22.83	1.48	21.32	1.45	17.66
High impact energy (6.2 J)	2.83	29.80	2.43	34.88	2.00	24.33

transversal yarn is not completely damaged, only several fibres. Thus, the depth of penetration is moderate. At high impact energies, tearing strength of transversal yarns are also exceeded by the impact force. Also, the fibres are not dishevelled; the cut is clear, see Fig. 11c (left).

- *Deformation:* Deformation of primary yarns occurs while secondary yarns are not cut as can be observed Fig. 11a (right). Penetrator pushes the fibres aside without cutting them. This mechanism was defined as windowing by Mayo et al.[14].
- *Mixed-failure mechanisms*: Penetrator edge begins to cut the yarns close to it. As knife penetrates, the secondary direction yarns are pushed. At low impact energies, Fig. 11b, the apparent hole or yarns displacement is more visible than those observed at high impact energies – Fig. 11c (centre). Once yarns are damaged, they provided little resistance to the knife penetration[16].

In other words, for low impact energies (Fig. 11a), there are two failure mechanisms: cutting yarns (left) and deformation (right). For moderate impact energies (Fig. 11b), the dominant failure mechanisms are: cutting yarns (left); and cutting yarns plus deformation (right). Finally, for high impact energies, the main failure mechanism found is fibre cutting (Fig. 11c).

Regarding **damage caused in TP-aramid**, Fig. 12 shows that it is prone to develop slitting line. However, as a consequence of SEM observations in TP-aramids, two different mechanisms are found in TP-aramids:

- *Petaling:* The knife pushes the TP-aramid to the side, causing woven bending and subsequent formation of symmetric petals as it is shown in Fig. 12a (left) and b. Therefore, deformation and rupture of primary and secondary yarns are carried out. The petalling mechanism has been observed up to 2.2 J impact energy.
- *Slitting line:* As mentioned above, this is the main failure mechanism produced by the stabbing process. Damage is along the breadth of the knife as shown Fig. 12a (right) and c. Damage on secondary yarns is neglected.

Also, SEM observations revealed that the TP-aramid held all its fibres together, resisting further penetration of knife.

The damaged area at each layer is analysed for all configurations (Fig. 13) in order to observe the influence of the laminate architecture. The analysis of material and its localization in the laminante is illustrated in (Fig. 14) to determine the best way to tailor the protection.

The application of optical procedure allowed obtaining the damaged area vs the impact energy (Fig. 13), increasing for the different configurations with the impact energy as it is expected. At low impact energies, the difference in damaged area between the three layers is negligible for all cases; however, at high impact energies, the difference increases up to 24% for all cases.

It is highlighted the behaviour of N-TP-N hybrid composite (Fig. 13b), where the first layer is N-aramid and reaches a value close to the maximum value around ≈2 J, remaining almost constant from this energy. From that point, the first layer seems to absorb less energy than the adjacent layers.

However, this behaviour is not observed in the first layer of TP-aramid in 3TP and TP-N-TP cases, Fig. 13a and c respectively. When TP-aramid is the first layer, damaged area increases with impact energy for impact energies considered and as is was observed in Fig. 6, the energy

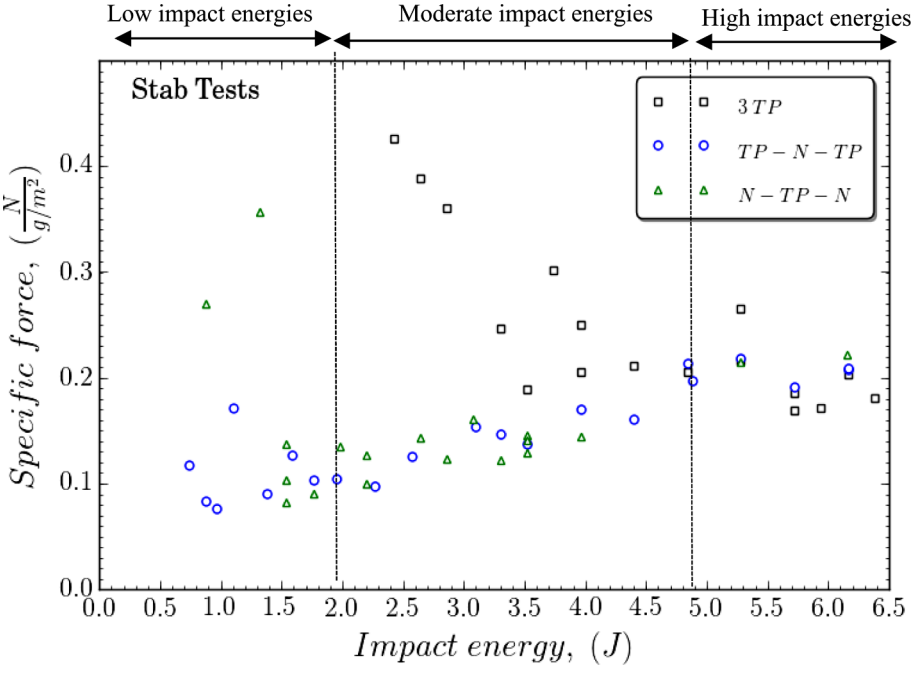

Fig. 9. Mean impact force of stab tests for each of laminate versus impact energy.

Table 5
Comparison of specific force.

	3 TP-aramid ($\rho_{areal} = 0.0952 g/cm^2$)	TP-N-TP aramid ($\rho_{areal} = 0.0698 g/cm^2$)	N-TP-N aramid ($\rho_{areal} = 0.0825 g/cm^2$)
Test	Specific force $\left(\frac{N}{g/m^2}\right)$	Specific force $\left(\frac{N}{g/m^2}\right)$	Specific force $\left(\frac{N}{g/m^2}\right)$
Moderate impact energy (2.4 J)	0.42	0.09	0.10
High impact energy (6.2 J)	0.18	0.20	0.22

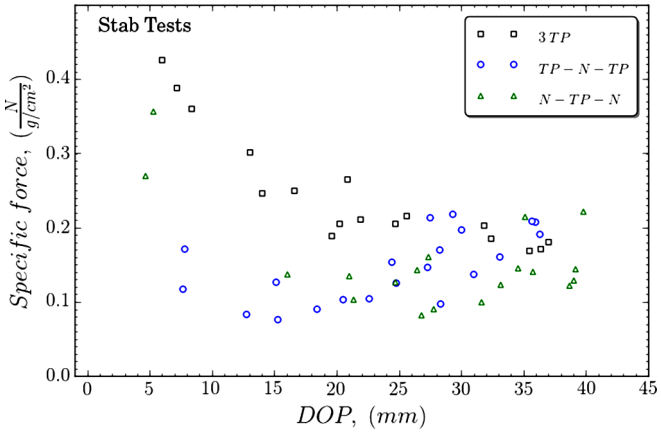

Fig. 10. Mean impact force of stab tests for each of laminate versus DOP.

absorbed by the laminate is also higher.

SEM observations also showed that the damaged area in 3TP composite (Fig. 13a) is higher than TP-N-TP hybrid composite (Fig. 13c) for all layers at high impact energies. The 3-TP composite may act as a block; in fact, the failure mechanisms are similar for all layers. Nevertheless, in case of TP-N-TP hybrid composite, the difference of damaged area between layers is higher. Therefore, N- aramid located in the middle of TP- aramids carries out a significant r eduction o f damaged area in the last layer.

To analyse the damaged area for every layer in each configuration, Fig. 14 is presented. In all cases, at low impact energies, N-aramid layer showed higher damage area than TP-aramid layers. Consequently, TP-aramid is interesting in order to reduce further damages and DOP. For this reason, TP- aramid acts as a protecting shield as Rao and collaborators demonstrated in[16]. However, this statement is not valid at high impact energies since TP-aramid shows less stabbing resistance at higher energies.

It is highlighted that N-aramid is the material that shows less damage area, Fig. 14b. Thus, the best localisation for N-aramid is in the middle of the laminate. The stiffer material (TP aramid) is commonly located as skins, and the softer material (N-aramid) is used in the core of sandwiches structures.

Regarding the third layer, at low impact energies, the difference in the damaged area between laminates is higher than in the case of high impact energies; as a matter of fact, the influence of the type of material used as the third layer is negligible in the considered range of impact energies, Fig. 14c.

4. Conclusions

In this paper, an experimental methodology to characterise the behaviour of different protective configurations under stabbing is presented. The importance of analysing a reduced number of plies with different stacking sequences was highlighted. Two woven aramid fabrics were considered: not treated N and thermoplastic TP aramid. Both provide interesting properties to the final performance of the protection. They were combined in three different architectures of three plies each: 3TP, and the hybrid configurations TP-N-TP and N-TP-N.

Experiments were based on conventional testing machines adapted to determine the stabbing resistance. From those tests, different parameters and variables were analysed. Particular attention was paid to those that take into account the different weight on the architectures

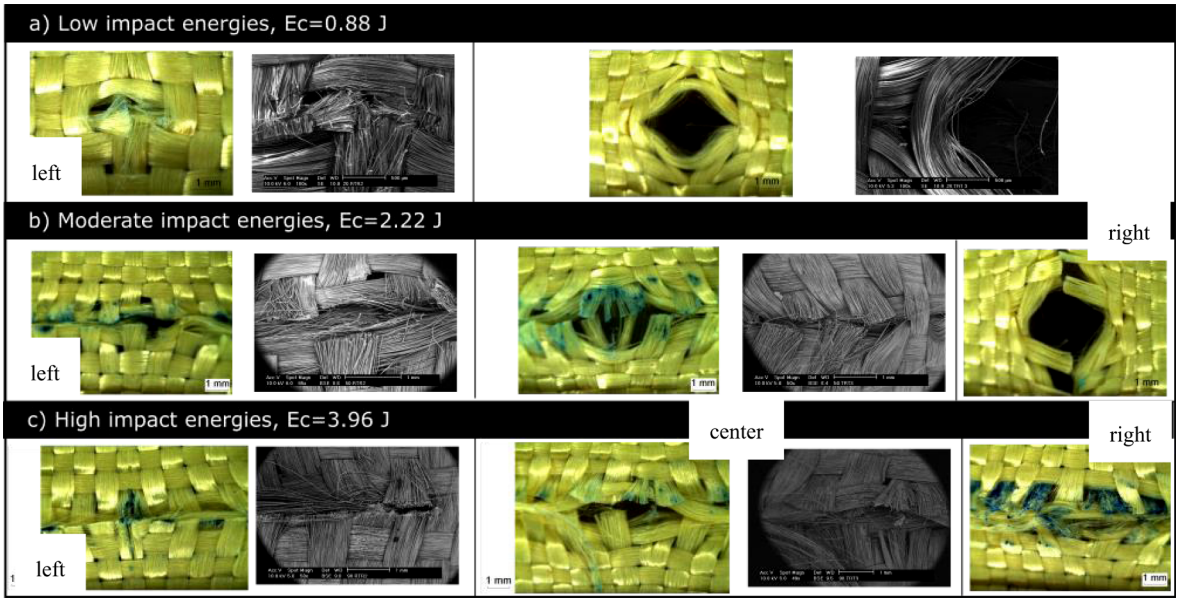

Fig. 11. N aramid: Main penetration mechanisms for several impact energies. a) $E_c = 0.88\,J$. b) $E_c = 2.22\,J$. c) $E_c = 3.96\,J$.

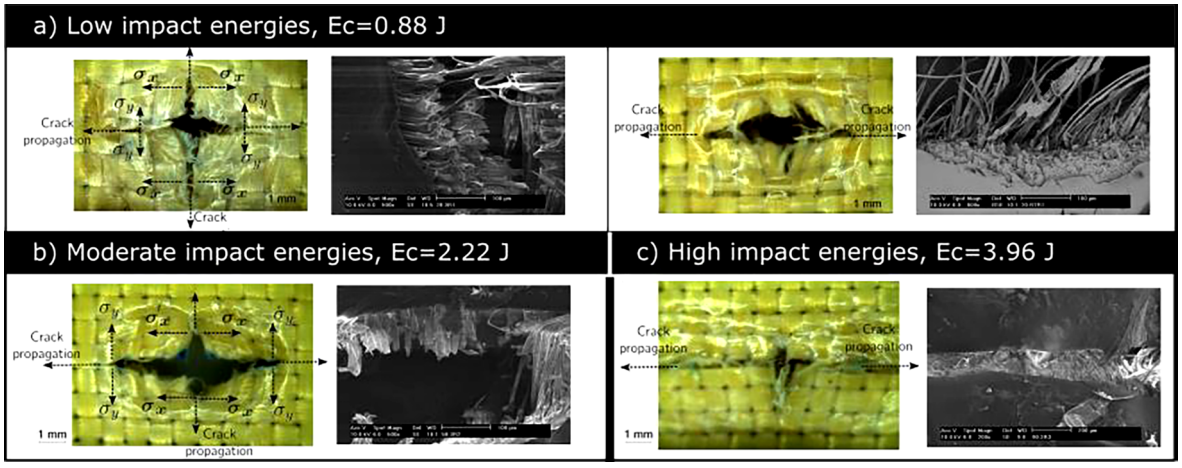

Fig. 12. TP aramid: Main penetration mechanisms for several impact energies. a) Ec = 0.88 J. b) Ec = 2.22 J. c) Ec = 3.96 J.

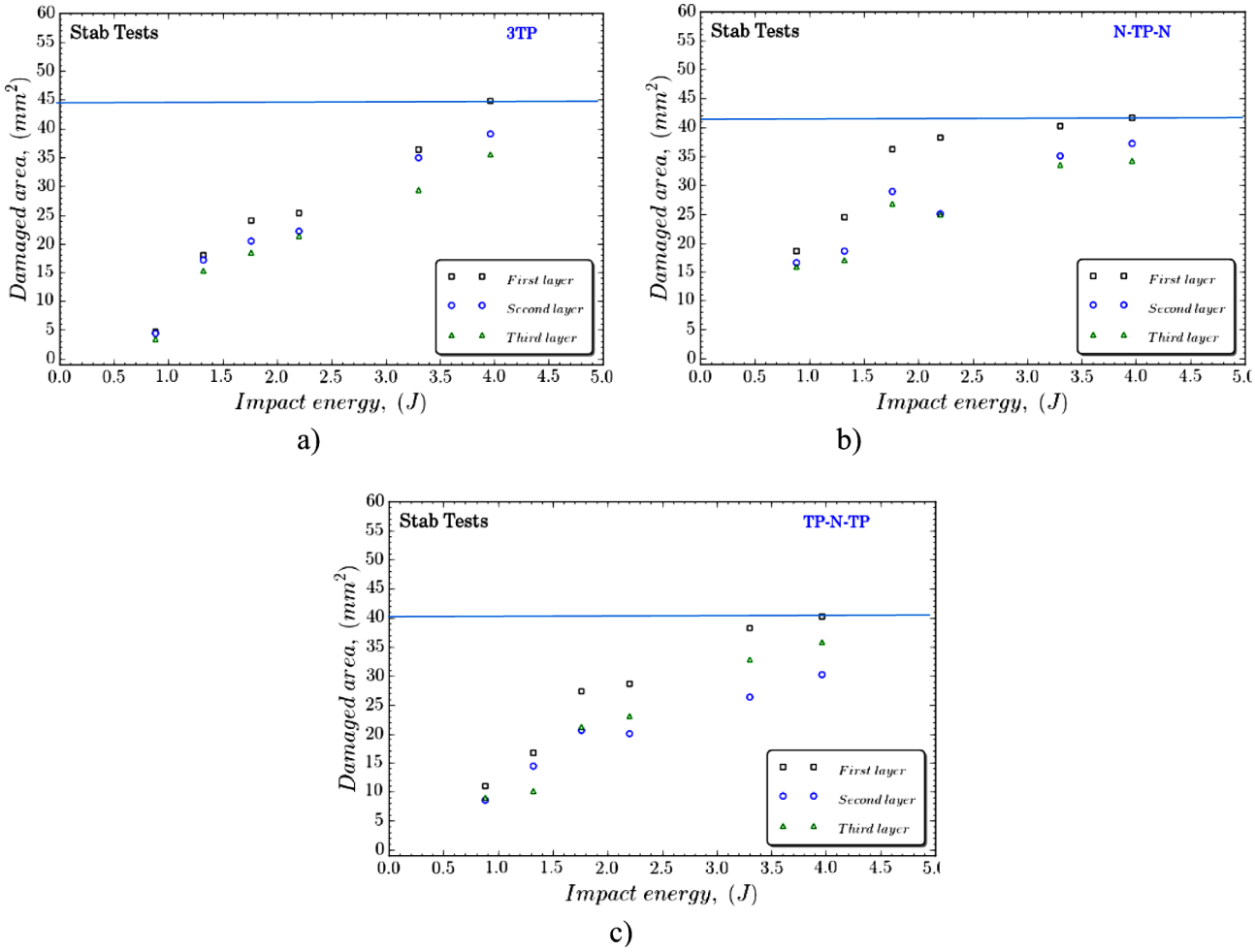

Fig. 13. Damage area on each layer in the different configurations: a) 3TP, b) N-TP-N hybrid composite and, c) TP-N-TP hybrid composite.

considered. From the analysis, it was determined that:

- The configuration TP-N-TP provides the maximum level of energy absorption per mass unit.
- The specific force is higher for the 3TP configuration at low values of impact energy. At high impact energies, the differences between the configurations become negligible.
- At a high level of impact energy, TP layer shows the largest damaged area.
- The use of N aramid acting as a core in the configuration TP-N-TP leads to a reduced damaged area in all layers.

In the range of impact energies analysed in this work, it can be concluded that the TP-N-TP protection is the best choice for stabbing protection with the advantage of including a flexible N layer also presenting lower areal density than TP layers. The methodology presented in this paper could help in the characterisation of protection materials before designing against a given threat. A detailed mechanical analysis

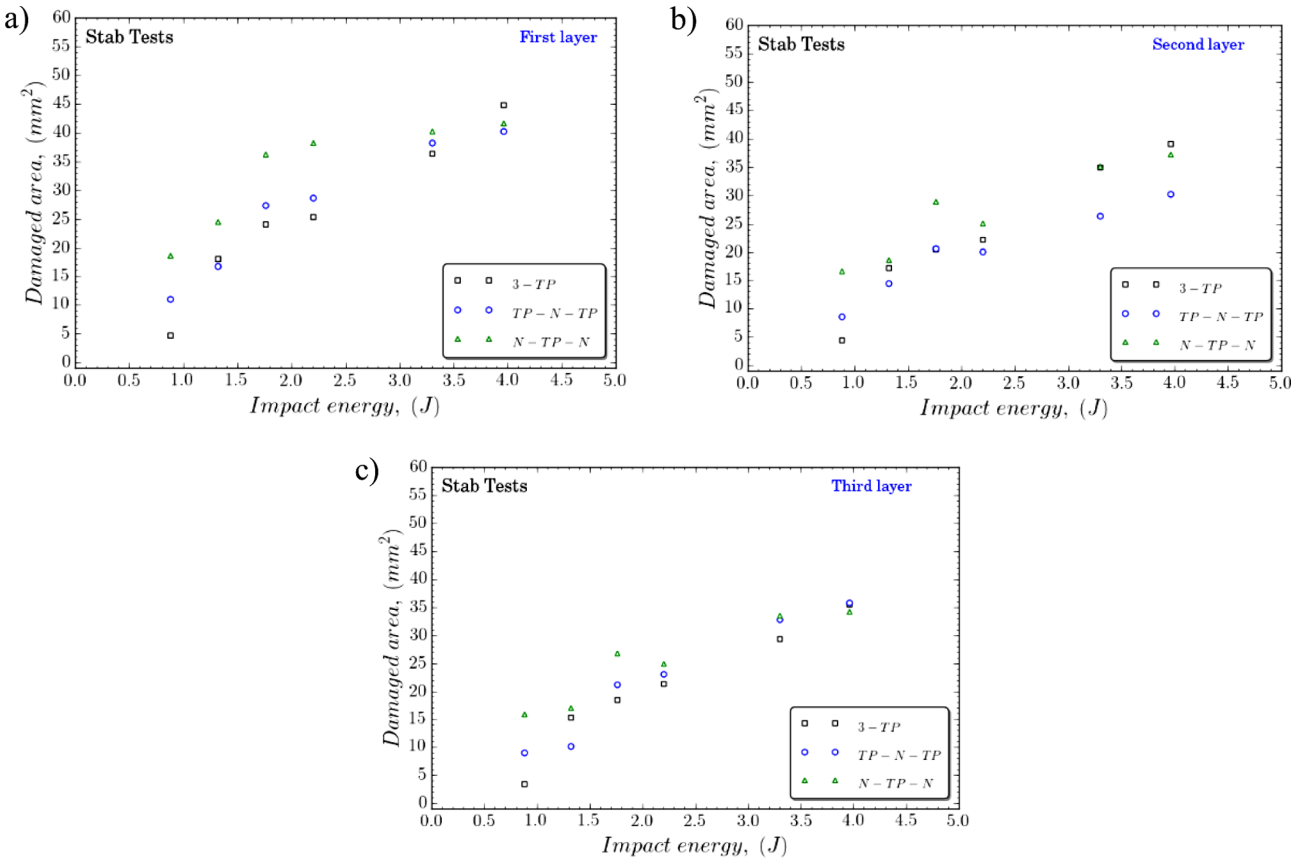

Fig. 14. Damage area on each layer a) first layer, b) the second layer and, c) the third layer.

should include more study variables, not just depth of penetration. The methodology presented in this work involves analysis of different parameters such as DOP, absorbed energy, impact force and the damaged area in the configurations.

Acknowledgements

The authors are indebted to the Spanish company FECSA for providing the tested aramids in the paper.

The authors acknowledge the Ministry of Economy and Competitiveness of Spain and FEDER program under the Project RTC-2015-3887-8 and the Project DPI2017-88166-R for the financial support of the work.

References

[1] Yang Y, Chen X. Study of energy absorption and failure modes of constituent layers in body armour panels. Compos Part B Eng 2016;98:250–9. https://doi.org/10.1016/j.compositesb.2016.04.071.

[2] Ha-Minh C, Imad A, Boussu F, Kanit T. Experimental and numerical investigation of a 3D woven fabric subjected to a ballistic impact. Int J Impact Eng 2016;88:91–101. https://doi.org/10.1016/j.ijimpeng.2015.08.011.

[3] Wang Y, Chen X, Young R, Kinloch I, Garry W. An experimental study of the effect of ply orientation on ballistic impact performance of multi-ply fabric panels. Text Res J 2015;68. https://doi.org/10.1177/0040517514566110.

[4] Shaktivesh Nair N, Naik N. Ballistic impact behavior of 2D plain weave fabric targets with multiple layers: analytical formulation. Int J Damage Mech 2015;24:116–50. https://doi.org/10.1177/1056789514524074.

[5] Luan K, Gu B. Energy absorption of three-dimensional angle-interlock woven composite under ballistic penetration based on a multi-scale finite element model. Int J Damage Mech 2015;24:3–20. https://doi.org/10.1177/1056789514520800.

[6] Pandya K, Kumar CVS, Nair N, Patil P, Naik N. Analytical and experimental studies on ballistic impact behavior of 2D woven fabric composites. Int J Damage Mech 2015;24:471–511. https://doi.org/10.1177/1056789514531440.

[7] Yuhazri M, Nadia NHC, Sihombing H, Yahaya SH, Abu A. A review on flexible thermoplastic composite laminate for anti-stab applications. J Adv Manuf Technol 2015;9:28.

[8] Kneubuehl. Wound Ballistics: Basics and Applications 2012. https://doi.org/10.1007/s00414-012-0744-0.

[9] Cowper EJ, Carr DJ, Horsfall I, Fergusson SM. The effect of fabric and stabbing variables on severance appearance. Forensic Sci Int 2015;249:214–24. https://doi.org/10.1016/j.forsciint.2015.01.024.

[10] Hejazi SM, Kadivar N, Sajjadi A. Analytical assessment of woven fabrics under vertical stabbing – the role of protective clothing. Forensic Sci Int 2016;259:224–33. https://doi.org/10.1016/j.forsciint.2015.12.036.

[11] Reiners P, Kyosev Y, Schacher L, Adolphe D, Kuster K. Experimental investigation of the influence of wool structures on the stab resistance of woven body armor panels. Text Res J 2015:1–11. https://doi.org/10.1177/0040517515596934.

[12] Barnat W, Sokolowski D, Gieleta R. Numerical and experimental research on stab resistance of a body armour package. Fibres Text East Eur 2014;22:90–6. https://doi.org/10.5604/12303666.1172090.

[13] Barnat W, Sokołowski D. The study of stab resistance of dry aramid fabrics. Acta Mech Autom 2014;8:53–8. https://doi.org/10.2478/ama-2014-0010.

[14] Mayo JB, Wetzel ED, Hosur MV, Jeelani S. Stab and puncture characterization of thermoplastic-impregnated aramid fabrics. Int J Impact Eng 2009;36:1095–105. https://doi.org/10.1016/j.ijimpeng.2009.03.006.

[15] Hosur MV, Mayo Jr. JB, Wetzel E, Jeelani S. Studies on the fabrication and stab resistance characterization of novel thermoplastic-kevlar composites. Solid State Phenom 2008;136:83–92. https://doi.org/10.4028/www.scientific.net/SSP.136.83.

[16] Rao H, Hosur M, Jr., Burton JM, Jeelani S, Stab S. Characterization of hybrid ballistic fabrics. In: Proc. SEM Annu. Conf.; 2009.

[17] Rao HM, Hosur MV, Jeelani S. Stab characterization of STF and thermoplastic-impregnated ballistic fabric composites. Adv Fibrous Compos Mater Ballist Prot Elsevier 2016:363–87. https://doi.org/10.1016/B978-1-78242-461-1.00012-1.[18] Zielinska D, Delczyk-Olejniczak B, Wierzbicki L, Wilbik-Hałgas BZE, Struszczyk MH, Leonowicz M. Investigation of the effect of para-aramid fabric impregnation with shear thickening fluid on quasi-static stab resistance. Text Res J 2014;84:1569–77. https://doi.org/10.1177/0040517514525881.

[19] NIST. Stab Resistance of Personal Body Armor, NIJ Standard-0115.00. Stab Resist Pers Body Armor, NIJ Stand 2000; JR000235.

[20] Crouch IG, Eu B. Ballistic testing methodologies. Sci Armour Mater Elsevier 2017:639–73. https://doi.org/10.1016/B978-0-08-100704-4.00011-6.

[21] Decker MJ, Halbach CJ, Nam CH, Wagner NJ, Wetzel ED. Stab resistance of shear thickening fluid (STF)-treated fabrics. Compos Sci Technol 2007;67:565–78. https://doi.org/10.1016/j.compscitech.2006.08.007.